

# Measurement-based Locational Marginal Prices for Real-time Markets in Distribution Systems

Roohallah Khatami, *Member, IEEE*, Severin Nowak, *Member, IEEE*, and Yu Christine Chen, *Member, IEEE*

**Abstract**—This paper presents a measurement-based method to calculate distribution locational marginal prices (DLMPs) toward establishing real-time electricity markets that help to support reliable and efficient operation of distribution systems. The calculation of DLMPs typically relies on an accurate and up-to-date distribution network model, but this may not be available in practice. Instead, central to the proposed method is the online estimation of linear sensitivity models that map bus voltages to power injections and to line power flows using *only* synchrophasor measurements collected at buses interfacing market participants and in lines of interest. The estimated linear models replace the nonlinear power flow constraints in a multi-period look-ahead optimal power flow (OPF) problem, thus obviating the need for an offline distribution network model in obtaining DLMPs as the optimal Lagrange multipliers of the linear sensitivity constraints. Moreover, the modified OPF problem with linear constraints is a convex quadratic programming problem, for which computationally efficient solvers are readily available. The resulting DLMPs also embed costs due to potential congestion in certain lines monitored by synchrophasor measurements. Numerical simulations demonstrate the effectiveness, adaptability, and scalability of the proposed measurement-based method to establish a real-time market for distributed generation, energy storage devices, and flexible loads.

**Index Terms**—Distribution system, electricity market, locational marginal price, measurement, synchrophasor

## I. INTRODUCTION

**E**XTENSIVE deployment of distributed energy resources (DERs), e.g., distributed generation, energy storage devices, and flexible loads, in power distribution networks is crucial in the transition to a low-carbon electric energy future. It is well recognized that benefits for grid operations can be realized via active coordination of DERs, enabling them to contribute to voltage support and congestion management [1]. Pivotal to broad adoption of these measures are electricity trading practices that can incentivize DERs to provide grid support and compensate them through a fair pricing scheme instead of payments based on fixed or time-of-use rates only [2]. Of particular interest for distribution networks are real-time markets (in the range of minutes to hours) as accurate longer-term forecasts of distributed generation and individual nodal loads needed for, e.g., day-ahead markets, may be more difficult to obtain [3]. A promising approach to establish distribution-level

real-time markets draws inspiration from wholesale electricity markets in the bulk transmission system, leading to the concept of distribution locational marginal prices (DLMPs) [4].

In general, given a forecast of nodal loads and bids from market participants over the scheduling horizon under consideration, calculating DLMPs involves repeated and rolling solutions of a multi-period look-ahead optimal power flow (OPF) problem. Distinct from the transmission-level pricing problem often formulated with lossless and linear power flow assumptions, the high resistance-to-reactance ratio typical of distribution networks calls for the inclusion of full-blown nonlinear power flow constraints, along with inter-temporal characteristics of energy storage devices and flexible loads, as well as operational limits related to DER capacities, line flows, and bus voltages. Due to the nonlinear and nonconvex nature of the resulting problem, the general approach may be computationally burdensome for practical deployment in large-scale distribution networks. Although various linearization and convexification techniques can offer computational savings, the solution approaches generally still require an accurate network model reflecting the up-to-date operating point, but this may not be available in real time [5]–[7]. The use of an inaccurate or outdated offline model may lead to erroneous DLMPs that do not support the market equilibrium, and accompanying decisions may result in suboptimal or undesirable system behaviour.

This paper proposes a measurement-based approach to overcome the aforementioned challenges. We extract DLMPs as the optimal Lagrange multipliers of estimated linear sensitivity-based equality constraints—replacing the nonlinear power flow equations—in the multi-period look-ahead OPF problem. The modified OPF problem with linear constraints is a convex quadratic programming problem, for which computationally efficient solution techniques are readily available. The linear constraints approximate the mapping from bus voltages to power injections, and we estimate the mapping on a rolling basis using *only* online measurements from synchrophasor technologies, e.g., distribution-level phasor measurement units (D-PMUs). In this way, the calculation of measurement-based DLMPs does not rely on any prior offline knowledge of the underlying network, and the resulting DLMPs adapt to the system’s evolving operating point and even changes in the network topology. The sampling and communication capabilities of D-PMUs ensure that the sensitivity model can be updated within a given market period to reflect the up-to-date system operating point [8]. With respect to measurement coverage, D-PMUs are needed only at buses that interface market participants, such as distributed generation (realized as dispatchable DERs), energy storage devices, and flexible loads.

Roohallah Khatami is with the Department of Electrical, Computer and Biomedical Engineering at Southern Illinois University, Carbondale, IL, USA. E-mail: roohallah.khatami@siu.edu. Severin Nowak is with the Lucerne University of Applied Sciences and Arts, Lucerne, Switzerland. E-mail: severin.nowak@hslu.ch. Yu Christine Chen is with the Department of Electrical and Computer Engineering at The University of British Columbia, Vancouver, Canada. E-mail: chen@ece.ubc.ca. The authors gratefully acknowledge the support of the Natural Sciences and Engineering Research Council of Canada (NSERC), funding reference number ALLRP 566892-21.

Compared with DLMPs calculated with exact (but outdated) nonlinear power flow constraints, the proposed measurement-based DLMPs solved from the modified OPF problem embedding an up-to-date (albeit linear) sensitivity model incur less computational burden and offer greater accuracy, even with relatively modest measurement coverage.

Prior work to address computational challenges associated with calculating DLMPs includes efforts to formulate the pertinent pricing problem by assuming radial topology and employing a relaxed convex branch-flow model [9]–[14]. Resulting DLMPs are applied to congestion management and voltage support [9], hierarchical economic dispatch involving distribution- and microgrid-network layers [10], pricing reactive power and ancillary services [11], and coordinating between transmission and distribution system operators [12]. Also, analytical properties of DLMPs obtained from the pricing problem formulated with a relaxed convex branch-flow model for radial networks are the focus of [13], [14]. However, the radial topology may be overly restrictive for future distribution networks with interconnected microgrids. Another general approach that is applicable for any network configuration leverages linear approximations in place of the nonlinear power flow constraints in the OPF problem, such as using the DC power flow approximation commonly invoked for transmission systems [15], computing line flows with a lossless line model and then lumping approximate losses as additional loads on either end of the line [16], and directly linearizing the nonlinear power flow equations around various operating points [17], [18]. While all methods in [9]–[18] tend to alleviate the computational burden of calculating DLMPs in radial or arbitrary networks, they all still depend on offline knowledge of (at least) the network topology, an up-to-date and accurate version of which may not be available in practice [5]–[7]. Meanwhile, the advancement of online measurement technologies motivates the development of data-driven approaches for power system operations, including methods to solve security-constrained economic dispatch [19], security-constrained OPF [20], and secure operation boundaries [21]. Furthermore, aimed at real-time decision making in the distribution network, our earlier work formulates a single-snapshot optimization problem intended to be solved every few seconds to determine the next optimal DER dispatch in a centralized [22] or distributed [23] manner. However, the aforementioned data-driven approaches focus on optimal decision making for (possibly security-aware) operations, and potential application to pricing is mentioned only in passing if at all.

This paper builds on preliminary work reported in [24] and provides extensions in several directions. First, the multi-period OPF problem formulated with inter-temporal constraints enables the inclusion of energy storage devices and flexible loads as market participants in addition to the dispatchable DERs considered in the simplified single-period formulation in [22]–[24]. This is consistent with current implementations of multi-period look-ahead scheduling and markets prevalent in the bulk transmission system, which serve as inspiration for establishing distribution-level markets rooted in locational marginal pricing. Further extending beyond [22]–

[24], we impose minimum and maximum flow limits on a subset of lines for which synchrophasor line active- and reactive-power flow measurements are available so that resulting measurement-based DLMPs embed congestion effects. Included as additional equality constraints in the OPF problem are linear sensitivity models that relate the pertinent line flows to bus voltages, which we also estimate on a rolling basis using online measurements only. We further provide extensive numerical simulations involving a 33-bus test system to demonstrate the effectiveness and adaptability of the resulting measurement-based DLMPs compared to their model-based counterparts for establishing real-time markets, especially in the presence of variations in operating point and changes in network topology. Finally, we report execution times involved with estimating the linear sensitivity models and solving the multi-period OPF in the proposed method for various numbers of market participants in an 874-bus test system.

The remainder of this paper is organized as follows. Section II outlines models for the distribution network and market participants along with the model-based multi-period look-ahead OPF problem to calculate DLMPs. In Section III, we present measurement-based DLMPs as the solution to a modified OPF problem that embeds an estimated sensitivity model as linear constraints in place of nonlinear power flow equations. Numerical simulations in Section IV demonstrate the effectiveness of the proposed measurement-based DLMPs. Finally, we provide concluding remarks in Section V.

## II. PRELIMINARIES

In this section, we describe models for the distribution network power flow and for DERs serving as market participants, including dispatchable DERs (representing distributed generation), energy storage devices, and flexible loads. We then formulate a general multi-period look-ahead OPF problem subject to nonlinear power flow constraints and various operational limits, the optimal solution of which includes model-based DLMPs. For the OPF problem, consider a scheduling horizon from time  $t_0$  to  $t_0 + T$ , where  $T$  is in the range of several hours. The scheduling horizon subdivides into multiple market periods of equal interval  $\Delta t$ , where  $\Delta t$  is in the range of 5 to 15 minutes. We collect end points of the market periods in the set  $\mathcal{T}_{t_0} = \{t_0 + \Delta t, t_0 + 2\Delta t, \dots, t_0 + T\}$ .

### A. Distribution Network Model

Consider a distribution system with  $N$  buses collected in the set  $\mathcal{N} = \{1, \dots, N\}$  and  $L$  transmission lines in the set  $\mathcal{L} = \{1, \dots, L\}$ . Suppose dispatchable DERs (representing distributed generation) are connected to  $G$  buses collected in the set  $\mathcal{G} \subseteq \mathcal{N}$ , energy storage devices are connected to  $S$  buses collected in the set  $\mathcal{S} \subseteq \mathcal{N}$ , flexible loads are connected to  $R$  buses collected in the set  $\mathcal{R} \subseteq \mathcal{N}$ , and inflexible loads are connected to all buses in  $\mathcal{N}$ . Without loss of generality, assume bus 1 is the substation, and further define the set  $\mathcal{N}^- = \mathcal{N} \setminus \{1\}$ . The substation power injection into the distribution feeder is modelled as the output of a dispatchable DER, so bus  $1 \in \mathcal{G}$  by default.

Let  $\theta_t = [(\theta_{i,t})_{i \in \mathcal{N}^-}]^T$  and  $V_t = [(V_{i,t})_{i \in \mathcal{N}^-}]^T$ , where  $\theta_{i,t}$  and  $V_{i,t}$  respectively denote the voltage phase angle and magnitude at bus  $i \in \mathcal{N}^-$  and at time  $t \in \mathcal{T}_{t_0}$ . Note that the substation is excluded from  $\theta_t$  and  $V_t$  as it represents the slack bus at which voltage is fixed and known. Then power flow equations can be compactly expressed as

$$P_t = f_t^P(\theta_t, V_t), \quad t \in \mathcal{T}_{t_0}, \quad (1)$$

$$Q_t = f_t^Q(\theta_t, V_t), \quad t \in \mathcal{T}_{t_0}, \quad (2)$$

where  $f_t^P : \mathbb{R}^{2N-2} \rightarrow \mathbb{R}^N$ ,  $f_t^Q : \mathbb{R}^{2N-2} \rightarrow \mathbb{R}^N$ , and the net bus active- and reactive-power injections are given by

$$P_t = W^g P_t^g + W^{\text{es}}(P_t^{\text{es,d}} - P_t^{\text{es,c}}) - W^f P_t^f - P_t^{\text{d}}, \quad (3)$$

$$Q_t = W^g Q_t^g + W^{\text{es}} Q_t^{\text{es}} - W^f Q_t^f - Q_t^{\text{d}}. \quad (4)$$

Above,  $P_t^g = [(P_{g,t}^g)_{g \in \mathcal{G}}]^T$  and  $Q_t^g = [(Q_{g,t}^g)_{g \in \mathcal{G}}]^T$  respectively collect active and reactive power produced by dispatchable DERs at time  $t \in \mathcal{T}_{t_0}$ ,  $P_t^{\text{es,c}} = [(P_{s,t}^{\text{es,c}})_{s \in \mathcal{S}}]^T$  ( $P_t^{\text{es,d}} = [(P_{s,t}^{\text{es,d}})_{s \in \mathcal{S}}]^T$ ) collects charging (discharging) active power from energy storage devices at time  $t \in \mathcal{T}_{t_0}$ ,  $Q_t^{\text{es}} = [(Q_{s,t}^{\text{es}})_{s \in \mathcal{S}}]^T$  collects reactive-power outputs from energy storage devices at time  $t \in \mathcal{T}_{t_0}$ , and  $P_t^f = [(P_{r,t}^f)_{r \in \mathcal{R}}]^T$  ( $P_t^{\text{d}} = [(P_{i,t}^{\text{d}})_{i \in \mathcal{N}}]^T$ ) and  $Q_t^f = [(Q_{r,t}^f)_{r \in \mathcal{R}}]^T$  ( $Q_t^{\text{d}} = [(Q_{i,t}^{\text{d}})_{i \in \mathcal{N}}]^T$ ) respectively collect active- and reactive-power withdrawals by flexible (inflexible) loads at time  $t \in \mathcal{T}_{t_0}$ . Furthermore,  $W^g \in \mathbb{R}^{N \times G}$ ,  $W^{\text{es}} \in \mathbb{R}^{N \times S}$ , and  $W^f \in \mathbb{R}^{N \times R}$  are matrices of 1s and 0s that map entries related to dispatchable DERs in  $\mathcal{G}$ , energy storage devices in  $\mathcal{S}$ , and flexible loads in  $\mathcal{R}$ , respectively, to corresponding bus indices in  $\mathcal{N}$ . Further define  $\pi_t = [(\pi_{\ell,t})_{\ell \in \mathcal{L}}]^T$  and  $\varphi_t = [(\varphi_{\ell,t})_{\ell \in \mathcal{L}}]^T$ , where  $\pi_{\ell,t}$  and  $\varphi_{\ell,t}$  respectively denote the active- and reactive-power flow in line  $\ell \in \mathcal{L}$  at time  $t \in \mathcal{T}_{t_0}$ . Given a particular power flow solution satisfying (1)–(2) at time  $t \in \mathcal{T}_{t_0}$ , we can express line active- and reactive-power flows compactly as follows:

$$\pi_t = h_t^P(\theta_t, V_t), \quad t \in \mathcal{T}_{t_0}, \quad (5)$$

$$\varphi_t = h_t^Q(\theta_t, V_t), \quad t \in \mathcal{T}_{t_0}, \quad (6)$$

where  $h_t^P : \mathbb{R}^{2N-2} \rightarrow \mathbb{R}^L$  and  $h_t^Q : \mathbb{R}^{2N-2} \rightarrow \mathbb{R}^L$ .

Here, it is important to note that, implicitly represented in the functions  $f_t^P(\cdot)$ ,  $f_t^Q(\cdot)$ ,  $h_t^P(\cdot)$ , and  $h_t^Q(\cdot)$  in (1)–(2) and (5)–(6) is the dependence on network parameters (such as circuit breaker status and line impedances) and any other power injections not explicitly modelled in (3)–(4). In general, these functions may vary over time due to, e.g., network topology reconfiguration or changes in other system parameters. We next outline models and constraints pertinent to dispatchable DERs, energy storage devices, and flexible loads.

## B. Market Participants

We consider distributed generation (realized as dispatchable DERs), energy storage devices, and flexible loads as market participants in the real-time distribution-level electricity market. Below, we describe their models and operational limits.

1) *Dispatchable DERs*: We model the active and reactive power produced by dispatchable DERs at time  $t \in \mathcal{T}_{t_0}$  as negative constant-power loads collected in  $P_t^g$  and  $Q_t^g$ , respectively. The substation bus is treated as a slack bus, which can be represented by a virtual DER, and its active- and reactive-power injections into the distribution feeder at time  $t \in \mathcal{T}_{t_0}$  appear as the first entries in  $P_t^g$  and  $Q_t^g$ , respectively. Power produced by dispatchable DERs are constrained to the following minimum and maximum limits:

$$\underline{P}^g \leq P_t^g \leq \overline{P}^g, \quad t \in \mathcal{T}_{t_0}, \quad (7)$$

$$\underline{Q}^g \leq Q_t^g \leq \overline{Q}^g, \quad t \in \mathcal{T}_{t_0}. \quad (8)$$

2) *Energy Storage Devices*: At time  $t \in \mathcal{T}_{t_0}$ , let  $E_t^{\text{es}} = [(E_{s,t}^{\text{es}})_{s \in \mathcal{S}}]^T$ , where  $E_{s,t}^{\text{es}}$  denotes the energy accumulated in energy storage device at bus  $s \in \mathcal{S}$ . The operational constraints of energy storage devices include the energy state

$$E_t^{\text{es}} = E_{t-\Delta t}^{\text{es}} + \left( \eta^c P_t^{\text{es,c}} - (\eta^{\text{d}})^{-1} P_t^{\text{es,d}} \right) \Delta t, \quad t \in \mathcal{T}_{t_0}, \quad (9)$$

where  $\eta^c$  and  $\eta^{\text{d}}$  are diagonal matrices of charging and discharging efficiency coefficients, respectively, and where  $E_t^{\text{es}}$  is constrained by

$$\underline{E}^{\text{es}} \leq E_t^{\text{es}} \leq \overline{E}^{\text{es}}, \quad t \in \mathcal{T}_{t_0}. \quad (10)$$

Energy storage devices are also subject to bounds in charging and discharging active power and in reactive-power outputs as

$$0 \leq P_t^{\text{es,c}} \leq \overline{P}^{\text{es,c}}, \quad t \in \mathcal{T}_{t_0}, \quad (11)$$

$$0 \leq P_t^{\text{es,d}} \leq \overline{P}^{\text{es,d}}, \quad t \in \mathcal{T}_{t_0}, \quad (12)$$

$$\underline{Q}^{\text{es}} \leq Q_t^{\text{es}} \leq \overline{Q}^{\text{es}}, \quad t \in \mathcal{T}_{t_0}. \quad (13)$$

3) *Flexible Loads*: Let  $P_t^{\text{des}} = [(P_{r,t}^{\text{des}})_{r \in \mathcal{R}}]^T$  and  $Q_t^{\text{des}} = [(Q_{r,t}^{\text{des}})_{r \in \mathcal{R}}]^T$ , where  $P_{r,t}^{\text{des}}$  and  $Q_{r,t}^{\text{des}}$  respectively denote the user's desired active- and reactive-power withdrawals by the flexible load at bus  $r \in \mathcal{R}$  and at time  $t \in \mathcal{T}_{t_0}$ . Further let  $E_t^{\text{dfc}} = [(E_{r,t}^{\text{dfc}})_{r \in \mathcal{R}}]^T$ , where the nonnegative  $E_{r,t}^{\text{dfc}}$  represents the energy deficit accumulated for the flexible load at bus  $r \in \mathcal{R}$  due to the mismatch in the scheduled load away from the corresponding desired value by time  $t \in \mathcal{T}_{t_0}$ . The accumulated energy deficit can be expressed as

$$E_t^{\text{dfc}} = E_{t-\Delta t}^{\text{dfc}} + (P_t^{\text{des}} - P_t^f) \Delta t, \quad t \in \mathcal{T}_{t_0}, \quad (14)$$

where the scheduled active-power load is constrained to

$$\underline{P}^f \leq P_t^f \leq \overline{P}^f, \quad t \in \mathcal{T}_{t_0}, \quad (15)$$

with  $\underline{P}^f$  and  $\overline{P}^f$  being informed by the flexible load's technical limits, such as the minimum and maximum charging rates for an electric vehicle. Flexible loads may also be bound to time deadlines that can be imposed on the energy deficit as

$$0 \leq E_t^{\text{dfc}} \leq \overline{E}_t^{\text{dfc}}, \quad t \in \mathcal{T}_{t_0}, \quad (16)$$

where the entry in  $\overline{E}_t^{\text{dfc}}$  pertinent to the flexible load connected to bus  $r \in \mathcal{R}$  is given by

$$\overline{E}_{r,t}^{\text{dfc}} = \begin{cases} 0, & \text{if } t = \tau_r, \\ +\infty, & \text{if } t \neq \tau_r, \end{cases} \quad (17)$$

implying that its energy deficit ought to be cleared by the specified deadline  $\tau_r$ . For example, an electric vehicle may need to be fully charged before a particular time. We assume that the scheduled reactive-power withdrawals from flexible loads  $Q^f$  follow similar changes as the scheduled active-power withdrawals, meaning that

$$(P_t^{\text{des}})^T \text{diag}(Q_t^f) = (Q_t^{\text{des}})^T \text{diag}(P_t^f), \quad t \in \mathcal{T}_{t_0}, \quad (18)$$

where  $\text{diag}(\cdot)$  denotes the diagonal matrix formed with the argument as the diagonal entries. It is worth noting that we utilize a queuing model for flexible loads, where  $P_t^{\text{des}}$  and  $P_t^f$  correspond to the arrival and departure components, respectively, and  $E_t^{\text{dfc}}$  represents the queue backlog. The constraint in (18) actualizes a joint queue for both active- and reactive-power withdrawals from flexible loads. Before moving on to formulate the model-based OPF problem, we mention that other market participants and quality of service constraints may be included, such as delay constraints for electric vehicles at public charging stations [25]. However, we refrain from offering an exhaustive selection to contain notational burden while spotlighting the main contributions.

### C. Model-based DLMPs and Problem Statement

In general, the DLMP at a bus represents the rate of change of optimal distribution system operation cost due to incremental changes in load at that bus [26]. Suppose we are furnished with a forecast of inflexible nodal active- and reactive-power loads  $P_t^d$  and  $Q_t^d$ , respectively, for  $t \in \mathcal{T}_{t_0}$ . With models for the distribution network power flow and market participants established previously, the DLMPs can be obtained alongside the optimal solution of the following multi-period look-ahead OPF problem:

$$\underset{\Omega}{\text{minimize}} \quad \sum_{t \in \mathcal{T}_{t_0}} C(P_t^g, Q_t^g) \quad (19a)$$

$$\text{subject to} \quad P_t = f_t^P(\theta_t, V_t), \quad t \in \mathcal{T}_{t_0}, \quad (\lambda_t), \quad (19b)$$

$$Q_t = f_t^Q(\theta_t, V_t), \quad t \in \mathcal{T}_{t_0}, \quad (\mu_t), \quad (19c)$$

$$\pi_t = h_t^P(\theta_t, V_t), \quad t \in \mathcal{T}_{t_0}, \quad (\alpha_t), \quad (19d)$$

$$\varphi_t = h_t^Q(\theta_t, V_t), \quad t \in \mathcal{T}_{t_0}, \quad (\beta_t), \quad (19e)$$

$$\underline{\pi} \leq \pi_t \leq \bar{\pi}, \quad t \in \mathcal{T}_{t_0}, \quad (\chi_t^-, \chi_t^+), \quad (19f)$$

$$\underline{\varphi} \leq \varphi_t \leq \bar{\varphi}, \quad t \in \mathcal{T}_{t_0}, \quad (\psi_t^-, \psi_t^+), \quad (19g)$$

$$\underline{V} \leq V_t \leq \bar{V}, \quad t \in \mathcal{T}_{t_0}, \quad (\nu_t^-, \nu_t^+), \quad (19h)$$

$$\text{DER power injection limits in (7)–(8),} \quad (19i)$$

$$\text{Energy storage model in (9)–(13),} \quad (19j)$$

$$\text{Flexible load model in (14)–(18),} \quad (19k)$$

where  $\Omega = \{\theta_t, V_t, \pi_t, \varphi_t, P_t^g, Q_t^g, P_t^{\text{es,c}}, P_t^{\text{es,d}}, Q_t^{\text{es}}, E_t^{\text{es}}, P_t^f, Q_t^f, E_t^{\text{dfc}}\}_{t \in \mathcal{T}_{t_0}}$  collects the decision variables over which the optimization is solved. The total operation cost of the distribution system is summed over the scheduling horizon for all  $t \in \mathcal{T}_{t_0}$  and minimized in the objective function (19a), which includes the cost to produce power from dispatchable DERs and to purchase power from the transmission system. The total cost is minimized subject to constraints pertinent to the network power flow in (19b)–(19e), as well as upper

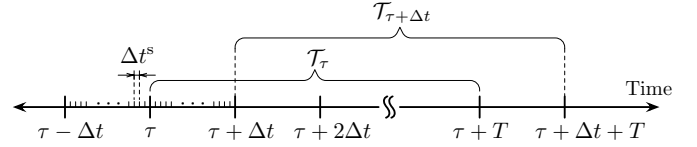


Fig. 1: Time scales involved with repeated and rolling instances of estimation and optimization in the proposed measurement-based market. As an example, at time  $\tau$ , we solve the measurement-based OPF problem in (24) with  $t_0 = \tau$  for the look-ahead scheduling horizon  $\mathcal{T}_\tau$  of length  $T$ . The OPF problem embeds an updated linear sensitivity model estimated using measurements collected at  $\Delta t^s$  intervals prior to time  $\tau$ . This procedure is repeated at time  $\tau + \Delta t$  for the look-ahead scheduling horizon  $\mathcal{T}_{\tau+\Delta t}$ , and so on. We consider  $\Delta t^s$ ,  $\Delta t$ , and  $T$  in the ranges of seconds, minutes, and hours, respectively.

and lower limits for line active- and reactive-power flows in (19f)–(19g) and bus voltages in (19h). Lagrange multipliers are included in parentheses after corresponding constraints. Additionally, models and constraints pertinent to dispatchable DERs, energy storage devices, and flexible loads are included in (19i), (19j), and (19k), respectively. Mathematically, the active-power (reactive-power) DLMP at a bus is the first derivative of the optimal Lagrangian of (19) with respect to the active-power (reactive-power) load at that bus [27]. Denote by  $\lambda_t^*$  and  $\mu_t^*$  the optimal values taken by Lagrange multipliers  $\lambda_t$  and  $\mu_t$ , respectively. Using the chain rule in calculus and the optimality conditions derived from the Karush-Kuhn-Tucker (KKT) conditions, it is straightforward to show that the  $i$ -th entry of  $\lambda_t^* \in \mathbb{R}^N$  ( $\mu_t^* \in \mathbb{R}^N$ ) represents the locational marginal price attributed to the active-power (reactive-power) load at bus  $i \in \mathcal{N}$  and at time  $t \in \mathcal{T}_{t_0}$ .

The OPF problem in (19) is constrained by exact power flow constraints, rendering the problem nonlinear and nonconvex. Hence, the calculation of DLMPs by solving (19) may incur significant computational burden incongruous with timelines accompanying fast changes in the electricity demand and generation expected at the grid edge. Although solving the OPF problem formulated with linearized or relaxed power flow constraints (see, e.g., [9]–[18]) helps to alleviate the computational burden, accurate DLMPs still rely on an offline system model that comprises the up-to-date network topology, line parameters, and operating point, which may not be available in practice [5]–[7]. In this paper, aimed at practical calculation of DLMPs for real-time markets with respect to both computational burden and reliance on offline models, we replace the nonlinear power flow constraints in (19b)–(19e) by linear sensitivity models estimated from *only* online synchrophasor measurements, obviating the need for any prior knowledge of the underlying physical network that is being measured.

## III. MEASUREMENT-BASED MARKET CLEARING

In this section, we describe the estimation of linear sensitivity models that then replace the nonlinear power flow equations in the multi-period look-ahead OPF problem. The solution of the modified OPF problem comprises measurement-based DLMPs alongside optimal setpoints for market participants. Figure 1 illustrates the time evolution of the proposed repeated and rolling instances of estimation and optimization.

### A. Estimating Linear Sensitivity Models

Let  $\mathcal{E} \subseteq \mathcal{N}$  represent the set of  $E$  buses in the distribution network equipped with D-PMUs. The calculation of measurement-based DLMPs at buses with market participants requires D-PMU measurements at these locations, so we assume that  $\mathcal{G} \cup \mathcal{S} \cup \mathcal{R} \subseteq \mathcal{E}$ . Additionally, it may be prudent to monitor buses that are at greater risk of violating operational constraints. Further let  $\mathcal{E}^- = \mathcal{E} \setminus \{1\}$ . Collect voltage phase angles and magnitudes of measured buses (except those of the substation where the voltage is assumed to be fixed and known) in vectors  $\theta_{\mathcal{E},t} = [(\theta_{i,t})_{i \in \mathcal{E}^-}]^T$  and  $V_{\mathcal{E},t} = [(V_{i,t})_{i \in \mathcal{E}^-}]^T$ , respectively. Also collect the inflexible active- and reactive-power loads at measured buses in vectors  $P_{\mathcal{E},t}^d = [(P_{i,t}^d)_{i \in \mathcal{E}}]^T$  and  $Q_{\mathcal{E},t}^d = [(Q_{i,t}^d)_{i \in \mathcal{E}}]^T$ , respectively. Net active- and reactive-power injections, collected in vectors  $P_{\mathcal{E},t} = [(P_{i,t})_{i \in \mathcal{E}}]^T$  and  $Q_{\mathcal{E},t} = [(Q_{i,t})_{i \in \mathcal{E}}]^T$  are then given by<sup>1</sup>

$$P_{\mathcal{E},t} = M^g P_t^g + M^{es} (P_t^{es,d} - P_t^{es,c}) - M^f P_t^f - P_{\mathcal{E},t}^d, \quad t \in \mathcal{T}_{t_0}, \quad (20)$$

$$Q_{\mathcal{E},t} = M^g Q_t^g + M^{es} Q_t^{es} - M^f Q_t^f - Q_{\mathcal{E},t}^d, \quad t \in \mathcal{T}_{t_0}, \quad (21)$$

where  $M^g \in \mathbb{R}^{E \times G}$ ,  $M^{es} \in \mathbb{R}^{E \times S}$ , and  $M^f \in \mathbb{R}^{E \times R}$  are matrices of 0s and 1s that map entries in  $\mathcal{G}$ ,  $\mathcal{S}$ , and  $\mathcal{R}$ , respectively, to the corresponding ones in  $\mathcal{E}$ . In addition to nodal quantities, we consider  $F$  particular lines in the set  $\mathcal{F} \subseteq \mathcal{L}$  that are equipped with flow measurements. These may include particularly sensitive transformers or lines requiring additional monitoring to ensure flow limits are not exceeded. The active- and reactive-power flows of measured lines are collected in  $\pi_{\mathcal{F},t} = [(\pi_{\ell,t})_{\ell \in \mathcal{F}}]$  and  $\varphi_{\mathcal{F},t} = [(\varphi_{\ell,t})_{\ell \in \mathcal{F}}]$ , respectively.

Suppose measurements of pertinent system variables are sampled at time  $t^s = k\Delta t^s$ ,  $k = 0, 1, \dots$ , where  $\Delta t^s$  is the sampling interval (in the range of several seconds or less [8]). For notational consistency, we distinguish measured or estimated values with  $\hat{\cdot}$  placed above corresponding variables. Collect measured bus voltage phase angles and magnitudes at time step  $k$  in  $\hat{x}_{\mathcal{E},t^s} = [\hat{\theta}_{\mathcal{E},t^s}^T, \hat{V}_{\mathcal{E},t^s}^T]^T$ . Further collect the measured net power injections (including those of the substation) and line power flows at time step  $k$  in  $\hat{y}_{\mathcal{E},t^s} = [\hat{P}_{\mathcal{E},t^s}^T, \hat{Q}_{\mathcal{E},t^s}^T]^T$  and  $\hat{z}_{\mathcal{F},t^s} = [\hat{\pi}_{\mathcal{F},t^s}^T, \hat{\varphi}_{\mathcal{F},t^s}^T]^T$ , respectively. We hypothesize a linear relationship between the measured injections/flows and voltages given by

$$\begin{bmatrix} \hat{y}_{\mathcal{E},t^s} \\ \hat{z}_{\mathcal{F},t^s} \end{bmatrix} = H_{t^s} \hat{x}_{\mathcal{E},t^s} + c_{t^s}, \quad (22)$$

where  $H_{t^s} \in \mathbb{R}^{2(E+F) \times 2(E-1)}$  and  $c_{t^s} \in \mathbb{R}^{2(E-1)}$  represent the linear- and constant-term coefficients, respectively. By collecting a minimum of  $2E$  most recent sets of measurements sampled in time and stacking the corresponding (transposed) instances of (22) while assuming  $H_{t^s}$  and  $c_{t^s}$  remain constant

<sup>1</sup>Throughout this paper, we routinely make use of  $w_i$  to denote the  $i$ th entry of vector variable  $w$ ,  $w_{i,t}$  to denote the value taken by  $w_i$  at time  $t$ , and  $w_t$  to denote the value taken by  $w$  at time  $t$ . Furthermore,  $w_{\mathcal{X}} = [(w_i)_{i \in \mathcal{X}}]^T$  collects entries in vector variable  $w$  for which corresponding indices belong to the set  $\mathcal{X}$ , and  $w_{\mathcal{X},t}$  denotes the value taken by  $w_{\mathcal{X}}$  at time  $t$ .

across these samples, it is straightforward to utilize the ordinary least squares (OLS) algorithm to obtain estimates of  $H_{t^s}$  and  $c_{t^s}$ , denoted by  $\hat{H}_{t^s}$  and  $\hat{c}_{t^s}$ , respectively. However, the OLS algorithm may lead to ill-conditioned regressor matrices due to correlation among voltages of nearby buses. The partial least squares (PLS) algorithm may be a promising alternative to overcome the collinearity problem and to provide meaningful estimates for  $\hat{H}_{t^s}$  and  $\hat{c}_{t^s}$  [22], [23]. We refer interested readers to [22] for further details on the PLS algorithm and its performance. For this paper, it suffices to assume that, at each sampling time step  $k$ ,  $\hat{H}_{t^s}$  and  $\hat{c}_{t^s}$  can be obtained using recent measurements via a suitable algorithm.

### B. Calculating Measurement-based DLMPs

To calculate measurement-based DLMPs, we modify the OPF problem in (19) in two ways. First, instead of assuming forecasts of inflexible loads are available at all buses, the modified OPF problem is solved with nodal loads forecasted at the measured buses only, i.e.,  $P_{\mathcal{E},t}^d$  and  $Q_{\mathcal{E},t}^d$ ,  $t \in \mathcal{T}_{t_0}$ . Inflexible loads at remaining buses are treated as unknown system parameters that may vary over time, and any such variations would be implicitly captured in the linear sensitivity models estimated using up-to-date online measurements. We also replace the nonlinear power flow constraints in (19b)–(19e) with estimated linear sensitivity models pertinent to the scheduling horizon beginning at time  $t_0$ , denoted by  $\hat{H}_{t_0}$  and  $\hat{c}_{t_0}$ , obtained via a suitable algorithm as mentioned in Section III-A. In practice, we advocate for using recently estimated models that would best reflect the up-to-date network topology and system operating point. Also, for the problem formulation and discussion to follow, we will find it useful to decompose  $\hat{H}_{t_0}$  and  $\hat{c}_{t_0}$  as

$$\hat{H}_{t_0} = \begin{bmatrix} \hat{J}_{t_0} \\ \hat{K}_{t_0} \end{bmatrix} = \begin{bmatrix} \hat{J}_{t_0}^{P\theta} & \hat{J}_{t_0}^{PV} \\ \hat{J}_{t_0}^{Q\theta} & \hat{J}_{t_0}^{QV} \\ \hat{K}_{t_0}^{P\theta} & \hat{K}_{t_0}^{PV} \\ \hat{K}_{t_0}^{Q\theta} & \hat{K}_{t_0}^{QV} \end{bmatrix}, \quad \hat{c}_{t_0} = \begin{bmatrix} \hat{b}_{t_0} \\ \hat{d}_{t_0} \end{bmatrix} = \begin{bmatrix} \hat{b}_{t_0}^P \\ \hat{b}_{t_0}^Q \\ \hat{d}_{t_0}^P \\ \hat{d}_{t_0}^Q \end{bmatrix}, \quad (23)$$

where the dimensions of submatrices are consistent with previously defined variables. For example, linear-term matrix coefficients include  $\hat{J}_{t_0} \in \mathbb{R}^{2E \times 2(E-1)}$ ,  $\hat{J}_{t_0}^{P\theta} \in \mathbb{R}^{E \times (E-1)}$ , and  $\hat{J}_{t_0}^{PV} \in \mathbb{R}^{E \times (E-1)}$ , and constant-term vector coefficients include  $\hat{b}_{t_0} \in \mathbb{R}^{2E}$  and  $\hat{d}_{t_0} \in \mathbb{R}^E$ .

With the above modifications to the OPF problem in (19) in mind, we formulate the measurement-based multi-period look-ahead OPF problem as follows:

$$\text{minimize} \quad \sum_{\Omega'} \sum_{t \in \mathcal{T}_{t_0}} C(P_t^g, Q_t^g) \quad (24a)$$

$$\text{subject to} \quad P_{\mathcal{E},t} = \hat{J}_{t_0}^{P\theta} \theta_{\mathcal{E},t} + \hat{J}_{t_0}^{PV} V_{\mathcal{E},t} + \hat{b}_{t_0}^P, \quad t \in \mathcal{T}_{t_0}, (\lambda'_t), \quad (24b)$$

$$Q_{\mathcal{E},t} = \hat{J}_{t_0}^{Q\theta} \theta_{\mathcal{E},t} + \hat{J}_{t_0}^{QV} V_{\mathcal{E},t} + \hat{b}_{t_0}^Q, \quad t \in \mathcal{T}_{t_0}, (\mu'_t), \quad (24c)$$

$$\pi_{\mathcal{F},t} = \hat{K}_{t_0}^{P\theta} \theta_{\mathcal{E},t} + \hat{K}_{t_0}^{PV} V_{\mathcal{E},t} + \hat{d}_{t_0}^P, \quad t \in \mathcal{T}_{t_0}, (\alpha'_t), \quad (24d)$$

$$\varphi_{\mathcal{F},t} = \hat{K}_{t_0}^{Q\theta} \theta_{\mathcal{E},t} + \hat{K}_{t_0}^{QV} V_{\mathcal{E},t} + \hat{d}_{t_0}^Q,$$

$$\begin{aligned}
t &\in \mathcal{T}_{t_0}, (\beta'_t), & (24e) \\
\pi_{\mathcal{F}} &\leq \pi_{\mathcal{F},t} \leq \bar{\pi}_{\mathcal{F}}, \quad t \in \mathcal{T}_{t_0}, (\chi'_t, \chi_t^+), & (24f) \\
\varphi_{\mathcal{F}} &\leq \varphi_{\mathcal{F},t} \leq \bar{\varphi}_{\mathcal{F}}, \quad t \in \mathcal{T}_{t_0}, (\psi'_t, \psi_t^+), & (24g) \\
V_{\mathcal{E}} &\leq V_{\mathcal{E},t} \leq \bar{V}_{\mathcal{E}}, \quad t \in \mathcal{T}_{t_0}, (\nu'_t, \nu_t^+), & (24h) \\
&\text{DER power injection limits in (7)–(8),} & (24i) \\
&\text{Energy storage model in (9)–(13),} & (24j) \\
&\text{Flexible load model in (14)–(18),} & (24k)
\end{aligned}$$

where  $\Omega' = \{\theta_{\mathcal{E},t}, V_{\mathcal{E},t}, \pi_{\mathcal{F},t}, \varphi_{\mathcal{F},t}, P_t^g, Q_t^g, P_t^{\text{es,c}}, P_t^{\text{es,d}}, Q_t^{\text{es}}, E_t^{\text{es}}, P_t^f, Q_t^f, E_t^{\text{dfc}}\}_{t \in \mathcal{T}_{t_0}}$  collects the decision variables in the optimization. The operation cost of the distribution system is minimized in the objective function (24a) subject to the estimated power flow constraints in (24b)–(24e), as well as upper and lower limits of measured line active- and reactive-power flows in (24f)–(24g) and measured bus voltages in (24h). Constraints pertinent to dispatchable DERs, energy storage devices, and flexible loads are reproduced from the model-based OPF problem in (19) as (24i), (24j), and (24k), respectively. Lagrange multipliers associated with different constraints in the modified OPF problem are included in parentheses thereafter.

Denote, by  $\lambda'_t$  and  $\mu'_t$ , the optimal values taken by Lagrange multipliers  $\lambda'_t$  and  $\mu'_t$ , respectively. Similar to the arguments made for the problem in (19), straightforward application of optimality conditions derived from the KKT conditions for the problem in (24) reveals that entries of  $\lambda'_t \in \mathbb{R}^E$  ( $\mu'_t \in \mathbb{R}^E$ ) represent the locational marginal prices attributed to the active-power (reactive-power) load at the corresponding buses and time  $t \in \mathcal{T}_{t_0}$ . Next, we establish conditions under which the measurement-based DLMPs coincide with their model-based counterparts via arguments based in optimality conditions.

### C. Drawing Connection to Model-based DLMPs

Recall  $\mathcal{E}$  collects buses that are equipped with D-PMUs. Further let  $\bar{\mathcal{E}} = \mathcal{N} \setminus \mathcal{E}$  collect unmeasured buses. Decompose net active-power (reactive-power) injections into measured and unmeasured components, i.e.,  $P_{\mathcal{E},t}$  and  $P_{\bar{\mathcal{E}},t}$  ( $Q_{\mathcal{E},t}$  and  $Q_{\bar{\mathcal{E}},t}$ ). Similarly decompose the voltage phase angles (magnitudes) into measured and unmeasured quantities, i.e.,  $\theta_{\mathcal{E},t}$  and  $\theta_{\bar{\mathcal{E}},t}$  ( $V_{\mathcal{E},t}$  and  $V_{\bar{\mathcal{E}},t}$ ). Further define measured variables  $y_{\mathcal{E},t} = [P_{\mathcal{E},t}^T, Q_{\mathcal{E},t}^T]^T$  and  $x_{\mathcal{E},t} = [\theta_{\mathcal{E},t}^T, V_{\mathcal{E},t}^T]^T$  and unmeasured variables  $y_{\bar{\mathcal{E}},t} = [P_{\bar{\mathcal{E}},t}^T, Q_{\bar{\mathcal{E}},t}^T]^T$  and  $x_{\bar{\mathcal{E}},t} = [\theta_{\bar{\mathcal{E}},t}^T, V_{\bar{\mathcal{E}},t}^T]^T$ . The optimal solution of the model-based OPF problem in (19) satisfies power flow equations in (1)–(2), reordered and decomposed into measured and unmeasured components as follows:

$$y_{\mathcal{E},t}^* = f_{\mathcal{E},t}(x_{\mathcal{E},t}^*, x_{\bar{\mathcal{E}},t}^*), \quad t \in \mathcal{T}_{t_0}, \quad (25)$$

$$y_{\bar{\mathcal{E}},t}^* = f_{\bar{\mathcal{E}},t}(x_{\mathcal{E},t}^*, x_{\bar{\mathcal{E}},t}^*), \quad t \in \mathcal{T}_{t_0}, \quad (26)$$

where  $f_{\mathcal{E},t}(\cdot)$  and  $f_{\bar{\mathcal{E}},t}(\cdot)$  consist of entries in  $[(f_t^P(\cdot))^T, (f_t^Q(\cdot))^T]^T$  corresponding respectively to measured and unmeasured buses. Also recall that  $\mathcal{F}$  collects lines that are equipped with flow measurements. By collecting active- and reactive-power flow variables pertinent to measured lines only into the vector  $z_{\mathcal{F},t} = [\pi_{\mathcal{F},t}^T, \varphi_{\mathcal{F},t}^T]^T$  and picking out

corresponding entries in (5)–(6), we can express these line flows at the optimal solution of (19) as

$$z_{\mathcal{F},t}^* = h_{\mathcal{F},t}(x_{\mathcal{E},t}^*, x_{\bar{\mathcal{E}},t}^*), \quad t \in \mathcal{T}_{t_0}, \quad (27)$$

where  $h_{\mathcal{F},t}(\cdot)$  comprises entries in  $[(h_t^P(\cdot))^T, (h_t^Q(\cdot))^T]^T$  corresponding to measured line active- and reactive-power flows.

**Proposition 1.** Given the optimal solution  $\Omega^*$  of the model-based problem in (19), measurement-based DLMPs coincide precisely with their model-based counterparts if

$$\hat{J}_{t_0} = J_{\mathcal{E}\mathcal{E},t}^* - J_{\mathcal{E}\bar{\mathcal{E}},t}^*(J_{\bar{\mathcal{E}}\bar{\mathcal{E}},t}^*)^{-1}J_{\bar{\mathcal{E}}\mathcal{E},t}^*, \quad \forall t \in \mathcal{T}_{t_0}, \quad (28)$$

$$\hat{b}_{t_0} = b_{\mathcal{E},t}^* + J_{\mathcal{E}\bar{\mathcal{E}},t}^*(J_{\bar{\mathcal{E}}\bar{\mathcal{E}},t}^*)^{-1}(y_{\bar{\mathcal{E}},t}^* - b_{\bar{\mathcal{E}},t}^*), \quad \forall t \in \mathcal{T}_{t_0}, \quad (29)$$

$$\hat{K}_{t_0} = K_{\mathcal{F}\mathcal{E},t}^* - K_{\mathcal{F}\bar{\mathcal{E}},t}^*(J_{\bar{\mathcal{E}}\bar{\mathcal{E}},t}^*)^{-1}J_{\bar{\mathcal{E}}\mathcal{E},t}^*, \quad \forall t \in \mathcal{T}_{t_0}, \quad (30)$$

$$\hat{d}_{t_0} = d_{\mathcal{F},t}^* + K_{\mathcal{F}\bar{\mathcal{E}},t}^*(J_{\bar{\mathcal{E}}\bar{\mathcal{E}},t}^*)^{-1}(y_{\bar{\mathcal{E}},t}^* - b_{\bar{\mathcal{E}},t}^*), \quad \forall t \in \mathcal{T}_{t_0}, \quad (31)$$

where Jacobian-type matrices are evaluated at the optimal solution of (19), as follows:

$$J_{\mathcal{E}\mathcal{E},t}^* = \left. \frac{\partial f_{\mathcal{E},t}}{\partial x_{\mathcal{E},t}} \right|_{(x_{\mathcal{E},t}^*, x_{\bar{\mathcal{E}},t}^*)}, \quad J_{\mathcal{E}\bar{\mathcal{E}},t}^* = \left. \frac{\partial f_{\mathcal{E},t}}{\partial x_{\bar{\mathcal{E}},t}} \right|_{(x_{\mathcal{E},t}^*, x_{\bar{\mathcal{E}},t}^*)}, \quad (32)$$

$$J_{\bar{\mathcal{E}}\mathcal{E},t}^* = \left. \frac{\partial f_{\bar{\mathcal{E}},t}}{\partial x_{\mathcal{E},t}} \right|_{(x_{\mathcal{E},t}^*, x_{\bar{\mathcal{E}},t}^*)}, \quad J_{\bar{\mathcal{E}}\bar{\mathcal{E}},t}^* = \left. \frac{\partial f_{\bar{\mathcal{E}},t}}{\partial x_{\bar{\mathcal{E}},t}} \right|_{(x_{\mathcal{E},t}^*, x_{\bar{\mathcal{E}},t}^*)}, \quad (33)$$

$$K_{\mathcal{F}\mathcal{E},t}^* = \left. \frac{\partial h_{\mathcal{F},t}}{\partial x_{\mathcal{E},t}} \right|_{(x_{\mathcal{E},t}^*, x_{\bar{\mathcal{E}},t}^*)}, \quad K_{\mathcal{F}\bar{\mathcal{E}},t}^* = \left. \frac{\partial h_{\mathcal{F},t}}{\partial x_{\bar{\mathcal{E}},t}} \right|_{(x_{\mathcal{E},t}^*, x_{\bar{\mathcal{E}},t}^*)}, \quad (34)$$

and constant terms are given by

$$b_{\mathcal{E},t}^* = y_{\mathcal{E},t}^* - J_{\mathcal{E}\mathcal{E},t}^*x_{\mathcal{E},t}^* - J_{\mathcal{E}\bar{\mathcal{E}},t}^*x_{\bar{\mathcal{E}},t}^*, \quad (35)$$

$$b_{\bar{\mathcal{E}},t}^* = y_{\bar{\mathcal{E}},t}^* - J_{\bar{\mathcal{E}}\mathcal{E},t}^*x_{\mathcal{E},t}^* - J_{\bar{\mathcal{E}}\bar{\mathcal{E}},t}^*x_{\bar{\mathcal{E}},t}^*, \quad (36)$$

$$d_{\mathcal{F},t}^* = z_{\mathcal{F},t}^* - K_{\mathcal{F}\mathcal{E},t}^*x_{\mathcal{E},t}^* - K_{\mathcal{F}\bar{\mathcal{E}},t}^*x_{\bar{\mathcal{E}},t}^*. \quad (37)$$

*Proof.* Linearization of (25)–(27) around the optimal solution of (19) yields the following approximation:

$$y_{\mathcal{E},t} \approx J_{\mathcal{E}\mathcal{E},t}^*x_{\mathcal{E},t} + J_{\mathcal{E}\bar{\mathcal{E}},t}^*x_{\bar{\mathcal{E}},t} + b_{\mathcal{E},t}^*, \quad t \in \mathcal{T}_{t_0}, \quad (38)$$

$$y_{\bar{\mathcal{E}},t} \approx J_{\bar{\mathcal{E}}\mathcal{E},t}^*x_{\mathcal{E},t} + J_{\bar{\mathcal{E}}\bar{\mathcal{E}},t}^*x_{\bar{\mathcal{E}},t} + b_{\bar{\mathcal{E}},t}^*, \quad t \in \mathcal{T}_{t_0}, \quad (39)$$

$$z_{\mathcal{F},t} \approx K_{\mathcal{F}\mathcal{E},t}^*x_{\mathcal{E},t} + K_{\mathcal{F}\bar{\mathcal{E}},t}^*x_{\bar{\mathcal{E}},t} + d_{\mathcal{F},t}^*, \quad t \in \mathcal{T}_{t_0}. \quad (40)$$

Straightforward algebraic manipulation of (38)–(40) yields

$$y_{\mathcal{E},t} \approx (J_{\mathcal{E}\mathcal{E},t}^* - J_{\mathcal{E}\bar{\mathcal{E}},t}^*(J_{\bar{\mathcal{E}}\bar{\mathcal{E}},t}^*)^{-1}J_{\bar{\mathcal{E}}\mathcal{E},t}^*)x_{\mathcal{E},t} + b_{\mathcal{E},t}^* + J_{\mathcal{E}\bar{\mathcal{E}},t}^*(J_{\bar{\mathcal{E}}\bar{\mathcal{E}},t}^*)^{-1}(y_{\bar{\mathcal{E}},t}^* - b_{\bar{\mathcal{E}},t}^*), \quad t \in \mathcal{T}_{t_0}, \quad (41)$$

$$z_{\mathcal{F},t} \approx (K_{\mathcal{F}\mathcal{E},t}^* - K_{\mathcal{F}\bar{\mathcal{E}},t}^*(J_{\bar{\mathcal{E}}\bar{\mathcal{E}},t}^*)^{-1}J_{\bar{\mathcal{E}}\mathcal{E},t}^*)x_{\mathcal{E},t} + d_{\mathcal{F},t}^* + K_{\mathcal{F}\bar{\mathcal{E}},t}^*(J_{\bar{\mathcal{E}}\bar{\mathcal{E}},t}^*)^{-1}(y_{\bar{\mathcal{E}},t}^* - b_{\bar{\mathcal{E}},t}^*), \quad t \in \mathcal{T}_{t_0}. \quad (42)$$

Recognizing the above, we find that the optimality conditions arising from the OPF problems in (19) and (24) are equivalent if (28)–(31) hold. In this case, the optimal solutions (including the DLMPs) of the two problems coincide precisely.  $\square$

The above implies that the optimality conditions of the model- and measurement-based OPF problems are equivalent if the estimated sensitivity model exactly coincides with the Kron-reduced first-order approximation of the nonlinear power flow equations with respect to voltage phase angles and magnitudes evaluated at the optimal solution.

#### D. Key Benefits and Potential Limitations

We next describe the benefits of the proposed measurement-based approach to calculate the DLMPs and highlight a few limitations inherent therein.

1) *Key Benefits*: The proposed approach does not rely on *any* prior offline knowledge of the underlying network, and it solves computationally tractable convex quadratic programming problems on a rolling basis. These benefits stem from the fact that the proposed method does not aim to estimate parameters in the physical circuit from which measurements are taken, but rather linear sensitivities relating voltages and injections at measured buses *only*. Assuming it is estimated correctly, the linear sensitivity model coincides exactly with the Kron-reduced first-order approximation of the nonlinear power flow equations with respect to voltage phase angles and magnitudes at measured buses, evaluated at the operating point from which measurements are obtained. This claim can be substantiated via a similar line of argument as the one used in Proposition 1. Furthermore, since an updated linear sensitivity model is estimated before each solution of the OPF problem in (24), the resulting DLMPs adapt to the system's evolving operating point and even changes in network topology, as we demonstrate via numerical case studies in Section IV. Another scenario to which the measurement-based DLMPs can adapt is the loss of a market participant at bus  $i$  and its measurements. After this contingency occurs,  $\mathcal{E}' = \mathcal{E} \setminus \{i\}$  would represent the set of  $E' = E - 1$  buses equipped with D-PMUs. The estimation and optimization stages of the proposed method would proceed as described in Sections III-A and III-B, respectively, except with  $\mathcal{E}$  and  $E$  replaced by  $\mathcal{E}'$  and  $E'$ , respectively. Here, the DLMPs at bus  $i$  would not accompany the solution of (24), but this is not an issue because the loss of the resource at bus  $i$  precludes it from participating in the market or being dispatched. Finally, the proposed measurement-based approach requires measurements at *only* buses with market participants in order to extract their nodal DLMPs. This criterion represents the minimum measurement coverage needed, and no additional measurements are needed to satisfy conditions related to, e.g., observability.

2) *Potential Limitations*: The conditions given in (28)–(31) are, in general, difficult to satisfy because we solve the modified OPF problem constrained by the *same* sensitivity models across the entire scheduling horizon and these sensitivity models are obtained at the beginning of the scheduling horizon *before* the optimal solution is realized. Particularly, errors in the measurement-based DLMPs may become more prominent if sufficiently drastic variations in the optimal operating point take place over the scheduling horizon. These essentially render the single measurement-based sensitivity model estimated before the scheduling horizon to be insufficient to approximate the power flow constraints across the entire scheduling horizon. Simulation results presented in Section IV-B support this hypothesis by showing mismatch between the proposed and benchmark methods in the market period immediately after a major network reconfiguration. During this market period, however, an updated linear sensitivity model representative of the reconfigured network topology is estimated, so

measurement-based DLMPs calculated in subsequent market periods match the benchmark model-based solution obtained with an accurate system model. In this way, repeated and rolling estimation of the sensitivity model followed by solution of the OPF problem (as depicted in Fig. 1) enable the proposed method to adapt to updated operating points within a few market periods. Stemming from the fact that the linear sensitivity model relates voltages and injections (or flows) at measured buses (or lines) only, another potential limitation of the proposed method is that it does not account for constraints in nodal voltages and line flows for unmeasured buses or lines. Similarly, it also does not incorporate potentially available load forecasts at unmeasured buses. In practice, we may wish to strategically place D-PMUs at buses or lines that are more likely to violate their limits, such as buses at the end of a feeder, in addition to buses connected to market participants.

#### IV. NUMERICAL SIMULATIONS

In this section, we demonstrate the effectiveness of the proposed measurement-based DLMPs toward establishing a real-time market for dispatchable DERs, energy storage devices, and flexible loads. We show that the measurement-based DLMPs are able to i) adapt to changes in topology and operating point, ii) closely match model-based solution obtained with an accurate system model, and iii) outperform the model-based solution obtained with an outdated model. Numerical case studies involve a 33-bus distribution network modified from the IEEE 33-bus test system (see, e.g., [28]). The single-line diagram of the test system is shown in Fig. 2. We consider two measurement coverage scenarios: i) full coverage with D-PMUs at all buses in  $\mathcal{E} = \{1, \dots, 33\}$ , and ii) partial coverage with D-PMUs at buses in the set  $\mathcal{E} = \{1, 3, 6, 7, 9, 11, 12, 15, 18, 19, 22, 25, 28, 31, 33\}$ , representing approximately 50% of all buses, including buses connected to all market participants as well as buses 9 and 31. We assume that D-PMUs provide synchronized measurements of voltage phase angles and magnitudes as well as net active- and reactive-power injections, all sampled at  $\Delta t^s = 5$  [sec] intervals.

##### A. Simulation Setup

For all  $t \in \mathcal{T}_{t_0}$ , the voltage magnitude at bus  $i \in \mathcal{E}$  is constrained to  $V_{i,t} \in [0.95, 1.05]$  [p.u.], and the substation bus voltage phase angle and magnitude are fixed at  $\theta_{1,t} = 0$  [rad] and  $V_{1,t} = 1$  [p.u.], respectively. As annotated in Fig. 2, the modified 33-bus test system includes dispatchable DERs connected to buses in  $\mathcal{G} = \{1, 6, 7, 12, 18, 22, 25, 33\}$  (including the substation bus), energy storage devices connected to buses in  $\mathcal{S} = \{11, 28\}$ , and flexible loads connected to buses in  $\mathcal{R} = \{3, 6, 12, 15, 18, 19, 22, 25\}$ . Parameters for the cost functions of dispatchable DERs (appearing in (19a) and (24a)) are reported in Appendix A.

For all  $t \in \mathcal{T}_{t_0}$ , the active- and reactive-power injections from the substation bus are respectively confined to  $P_{1,t}^g \in [-1, 1]$  [p.u.] and  $Q_{1,t}^g \in [-1, 1]$  [p.u.], and the active- and reactive-power outputs of the DER at bus  $g \in \mathcal{G}$  are respectively bounded by  $P_{g,t}^g \in [0, 0.12]$  [p.u.] and

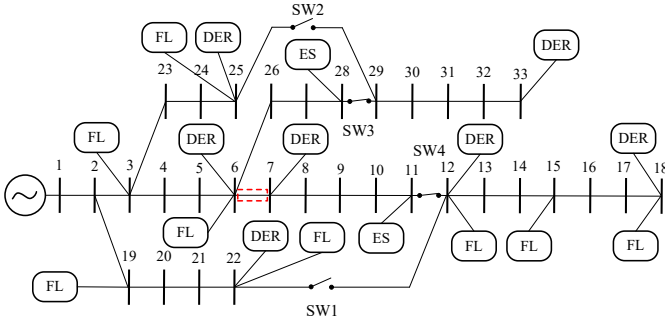


Fig. 2: One-line diagram for 33-bus test system modified to include dispatchable DERs, energy storage (ES) devices, and flexible loads (FLs). Bus 1 is assumed to be connected to a virtual DER. Switches SW1 and SW2 are normally open, and switches SW3 and SW4 are normally closed. The dashed box marks the line that becomes congested.

$Q_{g,t}^g \in [-0.012, 0.012]$  [p.u.]. For the energy storage device at bus  $s \in \mathcal{S}$ , the charging (discharging) active power is constrained within  $P_{s,t}^{\text{es},c} \in [0, 0.1]$  [p.u.] ( $P_{s,t}^{\text{es},d} \in [0, 0.1]$  [p.u.]), reactive power is set to  $Q_{s,t}^{\text{es}} = 0$  [p.u.], energy state is confined to  $E_{s,t}^{\text{es}} \in [0, 0.4]$  [p.u.], initial energy is set to  $E_{s,0}^{\text{es}} = 0$ , and charging and discharging efficiency coefficients are  $\eta_s^c = \eta_s^d = 0.95$ .

The total system active- and reactive-power loads are plotted in Fig. 3, and all nodal loads follow the same profile but scaled proportionally to their respective nominal values reported in [28]. At buses with flexible loads, the flexible component constitutes 20% of the total load at that bus, with the rest being inflexible. For the flexible load at bus  $r \in \mathcal{R}$ , the energy deficit should be cleared by the deadline  $\tau_r = 2.75$  [hr], and the scheduled active-power load is confined to  $P_{r,t}^f \in [0, 3 \times \max\{P_{r,t}^{\text{des}}\} | t \in \mathcal{T}_{t_0}]$ . Active- and reactive-power components of inflexible loads at all buses vary randomly around their nominal values as Gaussian distributed random variables with zero mean and 1% standard deviation relative to the respective nominal load values. Note that the nominal load values change over time following the trend shown in Fig. 3, and such changes would be reflected in measurements acquired afterward.

## B. Simulation Results

We consider a look-ahead scheduling horizon of  $T = 3$  [hr], starting at time  $t_0$ , which subdivides into  $|\mathcal{T}_{t_0}| = 12$  equal intervals of  $\Delta t = 15$  [min] each. Given a forecast of the inflexible components of active- and reactive-power loads connected to measured buses in the set  $\mathcal{E}$  for the next 3 [hr], the model- and measurement-based OPF problems in (19) and (24), respectively, are solved every 15 [min] on a rolling basis, i.e., at time  $t_0 = 0, 15, 30, \dots$  [min]. The rolling solutions consist of the optimal values for decision variables as well as accompanying DLMPs across the entire scheduling horizon of interest, but actually dispatched are DER setpoints from the first market period in each rolling scheduling horizon only, i.e., from time  $t_0$  to  $t_0 + \Delta t$ . We note that although we follow the market intervals and dispatch policy outlined above, the results presented in this section are typical in the sense that similar observations in comparing the proposed measurement-

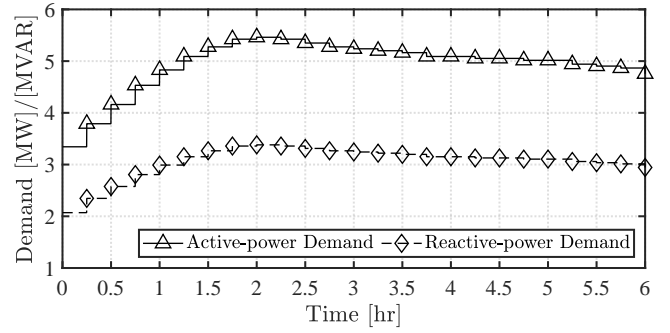


Fig. 3: Total active- and reactive-power load profile in the 33-bus test system.

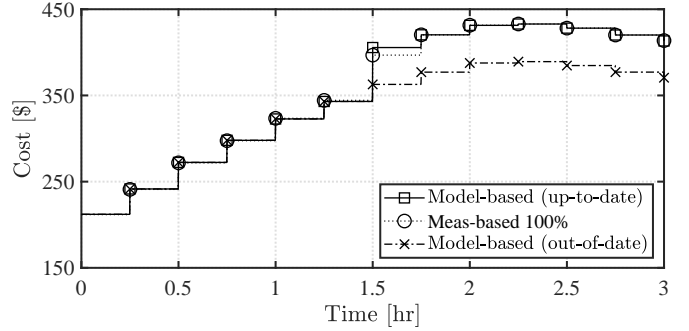


Fig. 4: Comparing operation costs obtained by solving i) the model-based OPF problem in (19) with accurate ( $\square$ ) and outdated ( $\times$ ) models, and ii) the measurement-based OPF problem in (24) with full measurement coverage ( $\circ$ ). Each step represents the cost incurred within the look-ahead scheduling horizon started from corresponding time interval, with change in network topology occurring at time 1 [hr] 16 [min].

based DLMPs to their model-based counterparts can be made for other policies as well.

Before solving each instance of the measurement-based OPF problem in (24), we estimate an up-to-date linear sensitivity model using synchrophasor measurements collected during the current 15 [min] market period via the PLS algorithm. We assume that the network topology changes at time 1 [hr] 16 [min] by closing the normally-open switches SW1 and SW2 and simultaneously opening the normally-closed switches SW3 and SW4. Afterward, we examine the solutions of the model-based OPF problem in (19) solved with i) the accurate *up-to-date* model, and ii) the *out-of-date* model assuming that the system operator is unaware of the network reconfiguration. In this comparison, the model-based DLMPs solved with an out-of-date model serve to underscore potential pitfalls of relying on an inaccurate offline model. The model-based nonlinear OPF problem is formulated as a second-order cone programming (SOCP) problem embedding relaxed branch flow equations and solved via the method described in [29]. We use Gurobi solver and extract the DLMPs as optimal Lagrange multipliers of the SOCP problem directly.

1) *Benchmark Comparisons*: Plotted in Fig. 4 are the operation costs resulting from rolling solutions of the model-based OPF problem embedding accurate and outdated models as well as the measurement-based OPF problem under full measurement coverage. The operation costs obtained by solving the measurement-based OPF problem closely follow the benchmark model-based solution except for the mismatch ob-

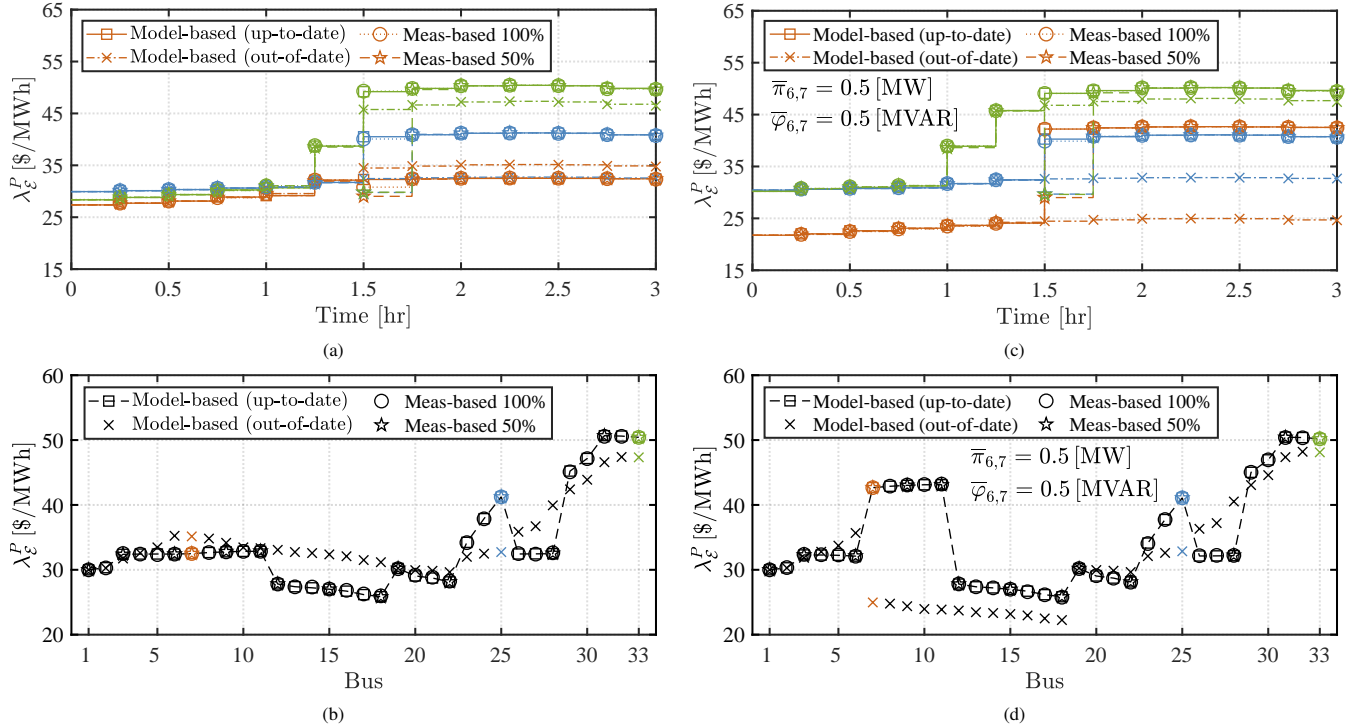


Fig. 5: Comparing active-power DLMPs obtained with (a)(b) nonbinding line flow constraints and (c)(d) binding flow constraints in the line connecting buses 6 and 7. Active-power DLMPs are solved from i) the model-based OPF problem in (19) with accurate ( $\square$ ) and outdated ( $\times$ ) models, and ii) the measurement-based OPF problem in (24) with 100% full ( $\circ$ ) and 50% partial ( $\star$ ) measurement coverage. (a)(c) Time-domain trajectories of DLMPs for buses 7 (orange colour), 25 (blue colour), 33 (green colour) with change in network topology occurring at time 1 [hr] 16 [min]. (b)(d) Snapshot of DLMPs for all buses taken at time 2 [hr] 15 [min].

served in the market period immediately following the network reconfiguration (i.e.,  $t \in [1.5, 1.75]$  [hr]). This mismatch stems from the linear sensitivity model used in the corresponding look-ahead measurement-based OPF, which is calculated using measurements collected before the network reconfiguration occurs. Later market periods are not affected because the sensitivity models are updated using measurements obtained after the reconfiguration. In contrast, the model-based solution obtained with an outdated model substantially underestimates the costs in all post-reconfiguration intervals. Extrapolating from this observation, the measurement-based method may perform poorly if major changes like network reconfiguration occur in every market period, so that even the newly estimated sensitivity model becomes outdated by the time the next look-ahead OPF problem is solved. In practice, however, we would not expect such major events to occur so frequently.

We examine the active-power DLMPs solved from the model-based (with accurate and outdated models) and measurement-based (under full and partial measurement coverage) OPF problems in Figs. 5a–5b. Specifically, Fig. 5a contains time-domain trajectories of active-power DLMPs at buses 7, 25, and 33, and Fig. 5b plots DLMPs at time 2 [hr] 15 [min] for all buses. Similar to operation costs, measurement-based DLMPs obtained under both full and partial measurement coverage are nearly identical to the benchmark model-based solution across the entire scheduling horizon except for a mismatch in the market period immediately following the reconfiguration, for the same reason articulated earlier. The snapshot of DLMPs at all buses presented in Fig. 5b further

showcase the accuracy of the proposed measurement-based DLMPs obtained at measured buses, outperforming the model-based method with an outdated model. Here, none of the line power flow limits are binding, so the variations observed among DLMPs at different buses are mainly due to line power losses and binding voltage constraints.

2) *Line Congestion*: We constrain active- and reactive-power flows in the line connecting buses 6 and 7 (marked by the dashed box in Fig. 2) to 0.5 [MW] and 0.5 [MVAR], respectively, in either direction. In the presence of binding line flow constraints, more pronounced variations are observed across DLMPs at different buses, as shown in Figs. 5c–5d, in comparison to those in Figs. 5a–5b. For example, the DLMPs at bus 7 depicted as the orange-coloured trace in Fig. 5c are considerably lower (higher) before (after) reconfiguration as compared to the corresponding trace in Fig. 5a. Also, time-sampled DLMPs at buses 7–11 shown in Fig. 5d are substantially higher than corresponding DLMPs at the same buses in Fig. 5b. The measurement-based DLMPs obtained under both full and partial measurement coverage effectively embed the impact of line congestion and provide accurate values for DLMPs compared to the model-based counterparts solved with an accurate model.

In Fig. 6, we plot the time-domain trajectories of active- and reactive-power flows in the line connecting buses 6 and 7 using optimal setpoints obtained from solving the model-based OPF problem (with accurate and outdated models) and measurement-based OPF problem under full measurement coverage. Under both binding and nonbinding line flow con-

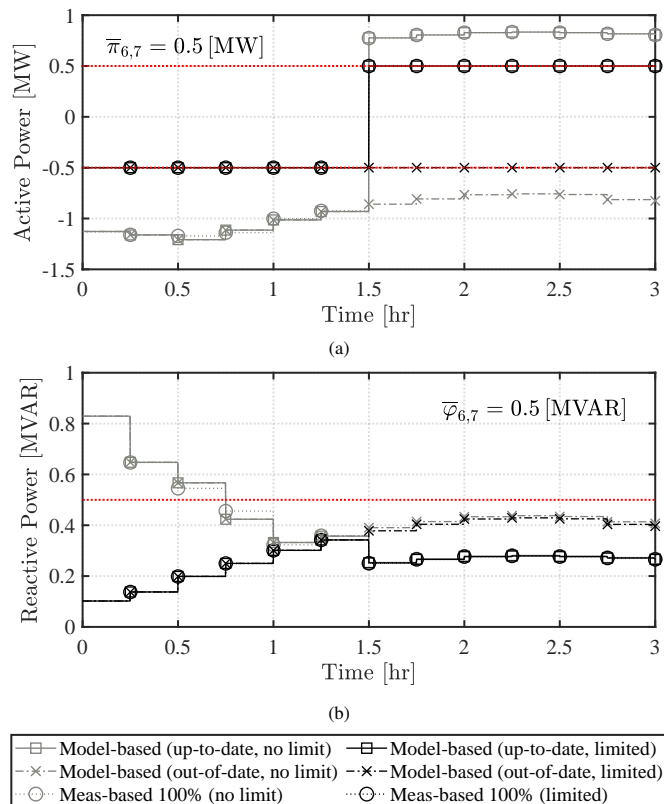


Fig. 6: (a) Active- and (b) reactive-power flows in the line connecting buses 6 and 7 where they are i) not limited and ii) limited to 0.5 [MW] and 0.5 [MVAR], respectively, in both directions. Upper and lower line flow limits are marked as red dotted traces.

straints, the measurement-based method effectively adapts to the topology change and provides optimal setpoints that result in the same power flows as solving the model-based OPF problem with an accurate model. In contrast, model-based setpoints solved with an outdated model leads to substantial error after the network reconfiguration. Furthermore, by imposing line flow limits, the active-power flow limit becomes binding in reverse (forward) direction before (after) reconfiguration, as shown by the trace corresponding to the benchmark model-based solution in Fig. 6a. The post-reconfiguration flows are perfectly replicated by the measurement-based method, but the model-based method is oblivious to even the change in power flow direction after reconfiguration. The measurement-based method performs similarly well for reactive-power flows.

Finally, it is worth mentioning that although we do not report directly on the optimal dispatch decisions, the proposed measurement-based method matches closely to the accurate model-based benchmark with similar trends as those observed in Figs. 4–6. We refer interested readers to our earlier work in [22], [23] focused on measurement-based optimal DER dispatch for more detailed comparisons.

### C. Execution Times

To assess the computational burden and the scalability of the proposed measurement-based framework, we report execution times involving the 874-bus test system from [30], in which up to 100 DERs are connected to arbitrary sets of

TABLE I: Execution times for estimating an up-to-date linear sensitivity model and solving one instance of the multi-period look-ahead OPF problem in (24), as well as the sum of the two stages, for different numbers of market participants in an 874-bus test system. Reported are per-solution values averaged across 12 look-ahead market runs.

Number of Market Participants	20	40	60	80	100
Estimation [s]	0.04	0.09	0.31	0.53	0.97
Optimization [s]	0.81	0.98	1.30	1.83	2.43
Total [s]	0.85	1.08	1.61	2.36	3.40

buses. In Table I, we report the execution times required for (i) estimating an up-to-date linear sensitivity model needed to construct the constraints in (24b)–(24e), (ii) solving one instance of the convex quadratic multi-period look-ahead OPF problem in (24) using Gurobi solver, and (iii) the sum of the estimation and optimization stages. Reported in Table I are per-solution values averaged across 12 look-ahead market runs. All solutions are performed in MATLAB R2022a on a personal computer with Intel Core i9-10900X processor at 3.70 GHz, and 32 GB RAM. We find that the proposed method can be executed well within the market interval of 15 [min] considered in Section IV-B for 100 market participants using the relatively limited computational resources available on a personal computer.

## V. CONCLUDING REMARKS

In this paper, we presented a measurement-based method to calculate DLMPs toward establishing real-time DER markets. Critical to the proposed method is replacing the nonlinear power flow equations in the pertinent multi-period look-ahead OPF problem by linear sensitivity models that are estimated using *only* online synchrophasor measurements of voltages and power injections at buses with market participants. The measurement-based DLMPs attributed to active and reactive power are respectively obtained as the optimal Lagrange multipliers of the estimated active- and reactive-power balance constraints. The measurement-based DLMPs also implicitly embed costs associated with congestion in lines of interest for which flow measurements are acquired. Extensive numerical simulations demonstrate the effectiveness of the proposed method to calculate accurate DLMPs at measured buses without relying on an up-to-date offline model of the distribution network. Compelling directions for future work include measurement-based pricing of combined energy and flexibility provided by DERs and distributed and privacy-preserving calculation of measurement-based DLMPs.

## APPENDIX

### A. Cost Function in (19a) and (24a)

In (19a) and (24a), we assume that the quadratic operation cost function takes the form  $C(P^g, Q^g) = P^{g\top} \text{diag}(a) P^g + b P^g + c$ , where  $a = [0, 1, 4, 2, 1.5, 2.5, 3.5, 4.5]$  [\$/ (MWh)<sup>2</sup>],  $b = [30, 10, 40, 20, 15, 25, 35, 45]$  [\$/MWh], and  $c = 0$  [\$/].

## REFERENCES

- [1] J. R. Aguero, E. Takayesu, D. Novosel, and R. Masiello, “Modernizing the grid: Challenges and opportunities for a sustainable future,” *IEEE Power & Energy Mag.*, vol. 15, no. 3, pp. 74–83, Apr. 2017.

- [2] O. W. Akinbode, *A distribution-class locational marginal price (DLMP) index for enhanced distribution systems*. Arizona State University, 2013.
- [3] R. Ulbricht, U. Fischer, W. Lehner, and H. Donker, "Optimized renewable energy forecasting in local distribution networks," in *Proc. the Joint EDBT/ICDT 2013 Workshops*, 2013, pp. 262–266.
- [4] P. M. Sotkiewicz and J. M. Vignolo, "Nodal pricing for distribution networks: efficient pricing for efficiency enhancing DG," *IEEE Trans. Power Syst.*, vol. 21, no. 2, pp. 1013–1014, May 2006.
- [5] J. Smith, B. Rogers, J. Taylor, J. Roark, B. Neenan, T. Mimmagh, and E. Takayesu, "Time and location: What matters most when valuing distributed energy resources," *IEEE Power and Energy Magazine*, vol. 15, no. 2, pp. 29–39, Mar. 2017.
- [6] A. Chapman, A. Fraser, L. Jones, H. Lovell, P. Scott, S. Thiebaut, and G. Verbic, "Network congestion management: Experiences from Bruny Island using residential batteries," *IEEE Power and Energy Magazine*, vol. 19, no. 4, pp. 41–51, Jun 2021.
- [7] M. Z. Liu, L. N. Ochoa, S. Riaz, P. Mancarella, T. Ting, J. San, and J. Theunissen, "Grid and market services from the edge: Using operating envelopes to unlock network-aware bottom-up flexibility," *IEEE Power and Energy Magazine*, vol. 19, no. 4, pp. 52–62, Jun 2021.
- [8] A. Von Meier, E. Stewart, A. McEachern, M. Andersen, and L. Mehrmanesh, "Precision micro-synchrophasors for distribution systems: A summary of applications," *IEEE Trans. Smart Grid*, vol. 8, no. 6, pp. 2926–2936, Nov. 2017.
- [9] L. Bai, J. Wang, C. Wang, C. Chen, and F. Li, "Distribution locational marginal pricing (DLMP) for congestion management and voltage support," *IEEE Trans. Power Syst.*, vol. 33, no. 4, pp. 4061–4073, Jul. 2018.
- [10] Z. Yuan, M. R. Hesamzadeh, and D. R. Biggar, "Distribution locational marginal pricing by convexified ACOPT and hierarchical dispatch," *IEEE Trans. Smart Grid*, vol. 9, no. 4, pp. 3133–3142, Jul. 2018.
- [11] J. Stekli, L. Bai, and U. Cali, "Pricing for reactive power and ancillary services in distribution electricity markets," in *Proc. 2021 IEEE Power & Energy Soc. Innov. Smart Grid Tech. Conf.*, 2021, pp. 1–5.
- [12] H. Chen, L. Fu, L. Bai, T. Jiang, Y. Xue, R. Zhang, B. Chowdhury, J. Stekli, and X. Li, "Distribution market-clearing and pricing considering coordination of DSOs and ISO: An EPEC approach," *IEEE Trans. Smart Grid*, Jul. 2021.
- [13] A. Papavasiliou, "Analysis of distribution locational marginal prices," *IEEE Trans. Smart Grid*, vol. 9, no. 5, pp. 4872–4882, Sep. 2018.
- [14] A. Winnicki, M. Ndrino, and S. Bose, "On convex relaxation-based distribution locational marginal prices," in *Proc. of 2020 IEEE Power & Energy Soc. Innov. Smart Grid Tech. Conf.*, 2020, pp. 1–5.
- [15] R. Li, Q. Wu, and S. S. Oren, "Distribution locational marginal pricing for optimal electric vehicle charging management," *IEEE Trans. Power Syst.*, vol. 29, no. 1, pp. 203–211, Jan. 2014.
- [16] H. Yuan, F. Li, Y. Wei, and J. Zhu, "Novel linearized power flow and linearized OPF models for active distribution networks with application in distribution LMP," *IEEE Trans. Smart Grid*, vol. 9, no. 1, pp. 438–448, Jan. 2016.
- [17] S. Hanif, K. Zhang, C. M. Hackl, M. Barati, H. B. Gooi, and T. Hamacher, "Decomposition and equilibrium achieving distribution locational marginal prices using trust-region method," *IEEE Trans. Smart Grid*, vol. 10, no. 3, pp. 3269–3281, May 2018.
- [18] M. Cai, R. Yang, and Y. Zhang, "Iteration-based linearized distribution-level locational marginal price for three-phase unbalanced distribution systems," *IEEE Trans. Smart Grid*, vol. 12, no. 6, pp. 4886–4896, Nov. 2021.
- [19] K. E. Van Horn, A. D. Domínguez-García, and P. W. Sauer, "Measurement-based real-time security-constrained economic dispatch," *IEEE Trans. Power Syst.*, vol. 31, no. 5, pp. 3548–3560, Sep. 2015.
- [20] F. Thams, L. Halilbasic, P. Pinson, S. Chatzivasileiadis, and R. Eriksson, "Data-driven security-constrained OPF," in *Proc. 10th Bulk Power Syst. Dyn. Control Symp.*, 2017, pp. 1–10.
- [21] J. L. Cremer, I. Konstantelos, S. H. Tindemans, and G. Strbac, "Data-driven power system operation: Exploring the balance between cost and risk," *IEEE Trans. Power Syst.*, vol. 34, no. 1, pp. 791–801, Jan. 2018.
- [22] S. Nowak, Y. C. Chen, and L. Wang, "Measurement-based optimal DER dispatch with a recursively estimated sensitivity model," *IEEE Trans. Power Syst.*, vol. 35, no. 6, pp. 4792–4802, Nov. 2020.
- [23] —, "Distributed measurement-based optimal DER dispatch with estimated sensitivity models," *IEEE Trans. Smart Grid*, vol. 13, no. 3, pp. 2197–2208, May 2022.
- [24] R. Khatami, S. Nowak, and Y. C. Chen, "Measurement-based locational marginal pricing in active distribution systems," in *IEEE Power & Energy Society General Meeting*, 2022.
- [25] K. Oikonomou, M. Parvania, and R. Khatami, "Deliverable energy flexibility scheduling for active distribution networks," *IEEE Trans. Smart Grid*, vol. 11, no. 1, pp. 655–664, Jul. 2019.
- [26] R. Khatami and M. Parvania, "Continuous-time locational marginal price of electricity," *IEEE Access*, vol. 7, pp. 129480–129493, Sep. 2019.
- [27] M. Parvania and R. Khatami, "Continuous-time marginal pricing of electricity," *IEEE Trans. Power Syst.*, vol. 32, no. 3, pp. 1960–1969, May 2016.
- [28] M. E. Baran and F. F. Wu, "Network reconfiguration in distribution systems for loss reduction and load balancing," *IEEE Trans. Power Del.*, vol. 4, no. 2, pp. 1401–1407, Apr. 1989.
- [29] M. Farivar and S. H. Low, "Branch flow model: Relaxations and convexification—part i," *IEEE Trans. Power Syst.*, vol. 28, no. 3, pp. 2554–2564, Apr. 2013.
- [30] H. Ahmadi, "874-node distribution test system," [http://www.ece.ubc.ca/~hameda/download\\_files/node\\_874.m](http://www.ece.ubc.ca/~hameda/download_files/node_874.m), online; Accessed: 2020-03-25.

**Roohallah Khatami** (Member, IEEE) received his B.Sc., M.S., and Ph.D. degrees respectively from Iran University of Science and Technology, Tehran, Iran, in 2007, Amirkabir University of Technology, Tehran, Iran, in 2013, and the University of Utah, Salt Lake City, UT, USA, in 2019, all in electrical engineering. He was a Postdoctoral Research Associate with the Department of Industrial & Systems Engineering, Texas A&M University, College Station, TX, USA, a Postdoctoral Research Fellow with the Department of Electrical and Computer Engineering, The University of British Columbia, Vancouver, BC, Canada, and he is currently an Assistant Professor in the School of Electrical, Computer, and Biomedical Engineering at Southern Illinois University at Carbondale, IL, USA. His research interests include power systems operation and electricity markets.

**Severin Nowak** (Member, IEEE) received a B.Sc. degree in electrical engineering from the University of Applied Sciences in Fribourg, Switzerland in 2008. He has received a Ph.D. degree from the School of Engineering, The University of British Columbia, Okanagan Campus in Kelowna, Canada, in 2021. He is currently a Lecturer and Scientist at Lucerne University of Applied Sciences and Arts, in Lucerne, Switzerland. His research interests are in the modernization of today's power grids, the deployment of renewable energy resources and integration of distributed assets with focus on data-driven approaches, and generally in initiatives towards a more sustainable energy future.

**Yu Christine Chen** (Member, IEEE) received the B.A.Sc. degree in engineering science from the University of Toronto, Toronto, ON, Canada, in 2009, and the M.S. and Ph.D. degrees in electrical engineering from the University of Illinois at Urbana-Champaign, Urbana, IL, USA, in 2011 and 2014, respectively. She is currently an Associate Professor in the Department of Electrical and Computer Engineering, The University of British Columbia, Vancouver, BC, Canada, where she is affiliated with the Electric Power and Energy Systems Group. Her research interests include power system analysis, operation, and control. Christine has served on the editorial boards of the *IEEE Transactions on Power Systems*, *IEEE Transactions on Energy Conversion*, and *IEEE PES Letters*.